

Emergence of robust gaps in 2D antiferromagnets via additional spin-1/2 probes

Aires Ferreira, J. Viana Lopes, and J. M. B. Lopes dos Santos¹

¹CFP and Departamento de Física, Faculdade Ciências Universidade do Porto, 687 4169-007, Porto, Portugal

We study the capacity of antiferromagnetic lattices of varying geometries to entangle two additional spin-1/2 probes. Analytical modeling of the Quantum Monte Carlo data shows the appearance of a robust gap, allowing a description of entanglement in terms of probe-only states, even in cases where the coupling to the probes is larger than the gap of the spin lattice and cannot be treated perturbatively. We find a considerable enhancement of the temperature at which probe entanglement disappears as we vary the geometry of the bus and the coupling to the probes. In particular, the square Heisenberg antiferromagnet exhibits the best thermal robustness of all systems, whereas the three-leg ladder chain shows the best performance in the natural quantum ground state.

PACS numbers:

I. INTRODUCTION

Solid-state systems have been exploited to integrate quantum information (QI) tasks and accomplish quantum computation in a single processing core, but many questions regarding their robustness against temperature and decoherence remain open. Among the requirements to achieve quantum computation, the ability to generate rapid elementary gates between well-characterized qubits is central [1]. In view of the technical difficulties of switching on direct interactions between qubits, various proposals have been put forward to use a quantum sub-system, usually denominated as *bus*, to mediate the fundamental universal gates [2, 3]. A considerable body of work has been devoted to chains of spins experiencing nearest-neighbor interactions, since they can be used as models for universal quantum computation, meeting the aforementioned requirements [4].

Spin chains are indeed a versatile laboratory for QI science for they naturally embody the SU(2) algebra of a qubit, allowing quantum information processing and manipulation along the traditional lines of quantum computing, that is, via the establishment of quantum gates [1]. In particular, numerical simulations [5] showed that spin systems can mediate entanglement between two spin probes separated by large distances, the so-called long-distance entanglement (LDE)—a quite remarkable phenomenon since, away from critical points, bulk correlations are completely classical at distances larger than a few sites [6]; gapless bosonic systems do not display this long distance entanglement capability [7].

The possibility of entangling spin systems via interaction with a larger system of spins was first pointed out by Chiara et al. in the proposal for entanglement extraction from solids [8]. Entanglement extraction from a large system might seem nonintuitive as generally the coupling to a system with many degrees of freedom leads unavoidably to decoherence [9]. However, a few notable exceptions are known: If two qubits, not interacting directly, are coupled in a symmetric way to a bath of harmonic oscillators, their entanglement will partially survive dur-

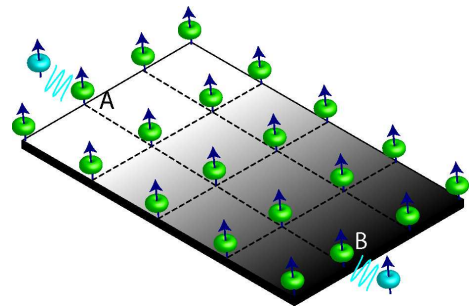


Figure 1: Schematic of the total system: The probes (blue) interact locally with a 2D lattice (the bus) through sites *A* and *B*. It is well known that spin chains can mediate entanglement between additional spin-1/2 particles, even at large distances [5, 16, 24] (the so-called LDE), but the question of how increasing dimensionality changes the 1D LDE picture has not been addressed until now.

ing their evolution when these qubits have degenerate energy eigenstates [10–12] or when the bath has a gap in its spectrum [13]. This is reminiscent of quantum computing using the so-called decoherence-free subspaces [14, 15].

Promising advances in the engineering of atomic structures and optical lattices, where finite spin systems are effectively realized in the laboratory, encourage the consideration of more general possibilities. In this article, we study the effect of adding two spin-1/2 probes to various antiferromagnetic spin-1/2 lattices, ranging from a one-dimensional chain to a two-dimensional (2D) antiferromagnetic (AF) lattice (the bus in QI terminology), on the probes LDE and spectrum. We confirm previous numerical results for the one-dimensional scenario [16] and extend this analysis to two dimensions via the first *direct* measure of probe correlation, with quantum Monte Carlo (QMC) methods. Our main findings are (1) an enhancement of LDE robustness regarding temperature in 2D AF Heisenberg systems, relative to the 1D chain; (2) the observation of a significant entanglement of the distant probes, even when the coupling to the bus is too strong to be described as a weak perturbation of the bus; and (3) the possibility of a complete

description of the temperature dependence of the entanglement of the probes in terms of a low energy manifold of singlet and triplet levels, with a large singlet-triplet gap, protecting probe entanglement from the undesirable effects of temperature—an unexpected phenomenon, especially for the square AF spin system, which *per se* has a vanishing gap and a broken symmetry phase in the thermodynamic limit [17]. This is a situation favorable to QI capabilities, particularly in the case of a 2D spin bus, where a relatively large singlet-triplet emerges with increasing probe-bus coupling, the singlet retaining significant probe-probe entanglement despite the stronger probe-bus coupling; we refer to this situation as presenting a “robust gap.”

The article is organized as follows. We start by making precise the conditions for a *robust gap* and set up the analytical theory which will allow us to conclude about the nature of the spectrum from the numerical simulations. The basic notions on LDE will also be reviewed (Sec. II). In Sec. III, the numerical results will be presented; in particular, (1) the singlet-triplet gap and LDE for all measured systems, (2) the robustness of thermal LDE in 2D, and (3) a surprisingly efficient entangler bus at $T = 0$, the three-leg ladder. We finish with conclusions and a discussion of consequences of the present work for LDE (Sec. IV). Details of derivations are presented in the appendices.

II. Analytical model

In this section, we introduce the analytical tools with which we modeled the Monte Carlo data. A few analytical results will be derived under the assumption of emergence of a *robust gap*. By this we mean the possibility of completely describing the probe’s entanglement, and its temperature variation, in terms of a low-lying singlet-triplet manifold which is isomorphic to the probe’s space of states. An analytical function, containing three parameters which are, in principle, calculable perturbatively, was found to fit the Monte Carlo data for probe entanglement almost perfectly.

A. Adiabatic continuity

We admit global $SU(2)$ symmetry of the couplings; more general types of interactions could be easily considered within this framework, but we focus on Heisenberg interactions, which not only allow universal quantum computation [3] but are also commonly realized in nature (e.g., in the parent compounds of copper-oxide high-temperature superconductors such as the undoped insulator La_2CuO_4 [17]; in electronically coupled quasi-1D chains such as the CuGeO_3 [18]; in the Mott insulating one-dimensional perovskite KCuF_3 [19]; and in linear

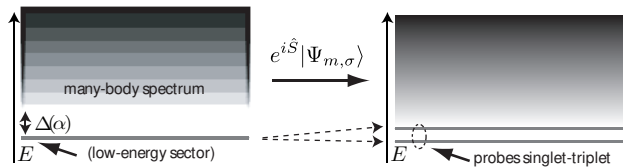


Figure 2: Schematic of the canonical transformed many-body spectrum (at right) under the assumptions of adiabatic continuity and a finite gap $\Delta(\alpha)$. If one succeeds in finding the matrix elements of \hat{S} , the low-energy physics of our problem will be described by an effective Hamiltonian containing just the probe’s canonical singlet and triplet states. The transformation \hat{S} renormalizes both operators and states.

chains of ~ 10 manganese atoms in engineered atomic structures [20]). We start by considering many-body systems of spins (which we will designate by bus) with rotational invariant Hamiltonian, H_0 , and a singlet, nondegenerate, ground state. Two probes, τ_a and τ_b (τ being the Pauli matrices), are coupled to the bus by Heisenberg exchange interaction with strength $J_p := J\alpha$, through sites A and B , respectively,

$$V = \alpha J \left(\vec{S}_A \cdot \vec{\tau}_a + \vec{S}_B \cdot \vec{\tau}_b \right), \quad (1)$$

where J denotes an energy scale of the bus (typically its exchange interaction), $\mathbf{S}_{A(B)} = (1/2)\tau_{A(B)}$, and α is a dimensionless parameter. We make the simple but crucial assumption that there is a one-to-one map of eigenstates of the uncoupled system ($\alpha = 0$) to the eigenstates of the full Hamiltonian; that is, we invoke adiabatic continuity [21]. Hence we define a canonical transformation between the two basis:

$$|\psi_m\rangle \otimes |\chi_\sigma^{ab}\rangle = e^{-i\hat{S}} |\Psi_{m,\sigma}\rangle, \quad (2)$$

where $|\psi_m\rangle$ is a bus-only eigenstate, $|\chi_\sigma^{ab}\rangle$ a probe state, and $|\Psi_{m,\sigma}\rangle$ an eigenstate for finite α . Note that the generator \hat{S} is an operator acting on both probe and bus space. This map has important consequences: The transformed Hamiltonian must have the form of a sum of a probe-only term (H_p) with a bus-only term (H'_b), that is, $H \rightarrow H_p + H'_b$, since the corresponding eigenstates are product states. We now add the assumption that the lowest lying states which map to a probe singlet and probe triplet,

$$|\Psi_{0,s}\rangle = e^{i\hat{S}} |\psi_0\rangle \otimes |\chi^s\rangle, \quad (3)$$

$$|\Psi_{0,m}\rangle = e^{i\hat{S}} |\psi_0\rangle \otimes |\chi^t_m\rangle \quad m = 0, \pm 1, \quad (4)$$

respectively, are well-separated from states which map to excited states of the bus by a finite gap, $\Delta(\alpha)$. In the scenario we have in mind—and which is confirmed by the simulations—entanglement between the probes

disappears well before significant thermal occupation of states above $\Delta(\alpha)$ occurs. But an important remark is in order: While the probes are obviously entangled in the state $|\chi^s\rangle$, it is the entanglement in the state $|\Psi_{0,s}\rangle$ which matters. In other words, the canonical transformation changes operators as well as states; if we are to use the transformed uncoupled basis in the calculation, the probe entanglement *is* not the entanglement of τ_a and τ_b , but rather the entanglement of the renormalized spins,

$$\tau_{a(b)}^R := e^{-i\hat{S}} \tau_{a(b)} e^{i\hat{S}}. \quad (5)$$

We now proceed to use this concept of adiabatic continuity to develop a description of the probe-reduced density matrix.

B. Robust gap and canonical corrections.

The exact density matrix of the qubits (the partial state of the probes, ρ_{ab}) encodes the full capabilities of a generic lattice as a quantum bus (in particular, the possibility of LDE) and is given by the Gibbs canonical state

$$\rho_{ab} = \mathcal{Z}_{ab}^{-1} \text{Tr}_{i \in \mathcal{L}} \left[e^{-\beta(H_0 + V)} \right]. \quad (6)$$

The trace is made with respect to the degrees of freedom of the bus, \mathcal{L} , and $\mathcal{Z}_{ab} = \text{Tr}[\exp(-\beta H_0 - \beta V)]$ is the system's partition function. In our case, global $SU(2)$ symmetry implies a very simple form for ρ_{ab} ,

$$\rho_{ab} \propto \exp[-\beta J_{ab}(\beta) \tau_a \cdot \tau_b], \quad (7)$$

where $J_{ab}(\beta)$ is the actual effective coupling of the probes and depends upon the temperature, as a consequence of tracing out the degrees of freedom of \mathcal{L} . If this function is known, bipartite entanglement can be computed using the negativity [22], the concurrence [23], or any other entanglement monotone. For systems with full rotational symmetry entanglement, bipartite entanglement $[E(\rho_{ab})]$ is a function of the probe correlation,

$$\langle \tau_a \cdot \tau_b \rangle = \text{Tr}[\rho_{ab} \tau_a \cdot \tau_b] = \frac{e^{-4\beta J_{ab}(\beta)} - 1}{e^{-4\beta J_{ab}(\beta)} + 1/3}. \quad (8)$$

The concurrence E_C is of particular simplicity for rotational $2 \otimes 2$ systems,

$$E_C(\rho_{ab}) = \max \left[0, \left| \frac{\langle \tau_a \cdot \tau_b \rangle}{3} \right| - \frac{\langle \tau_a \cdot \tau_b \rangle + 3}{6} \right] \in [0, 1]. \quad (9)$$

The probes will be entangled whenever $E_C(\rho_{ab}) > 0$, which happens for strong AF correlations, more precisely, when $\langle \tau_a \cdot \tau_b \rangle < -1$. One straightforwardly derives the critical temperature, $T_c \equiv 1/\beta_c$, above which entanglement vanishes for the state (7). It reads,

$$\beta_c J_{ab}(\beta_c) \simeq 0.27. \quad (10)$$

One speaks about long-distance entanglement whenever $E(\rho_{ab}) > 0$ for probes distances of the order of the system size. In the remainder of this section, we present the analytical form of $J_{ab}(\beta)$, under the assumption of a robust gap.

In [24], the authors derived the effective probe interaction H_{eff} for probes weakly coupled to a large system with a gap to the first excited state, $\Delta_0 \equiv \Delta(\alpha = 0) > 0$. For $SU(2)$ symmetric couplings, it reads as follows,

$$H_{\text{eff}} = \alpha^2 J^2 \tilde{\chi}_r(0) \tau_a \cdot \tau_b, \quad (11)$$

where $\tilde{\chi}_r(0)$ is the Fourier transform at zero frequency of the adiabatic spin susceptibility defined as $\chi_r(t) = -i \langle [S_0^z(t), S_r^z] \rangle \theta(t)$, with $\theta(t)$ being the Heaviside function and r the distance between spins A and B in the lattice. The effective Hamiltonian (11) holds strictly when,

$$J_{\text{eff}} := \alpha^2 J^2 \tilde{\chi}_r(0) \ll \Delta_0, \quad (12)$$

and correctly describes the low-lying spectrum in that limit. However, as remarked previously, one should be careful in using this Hamiltonian to calculate probe correlations [24]. Consider, for instance, the zero-temperature limit. Assuming a system with AF correlations [$\tilde{\chi}_r(0) > 0$], according to Eq. (11), we have,

$$\langle \tau_a \cdot \tau_b \rangle = \frac{1}{\mathcal{Z}_{ab}} \text{Tr} \left[\tau_a \cdot \tau_b e^{-\beta \alpha^2 J^2 \tilde{\chi}_r(0) \tau_a \cdot \tau_b} \right] \xrightarrow{\beta \rightarrow \infty} -3, \quad (13)$$

in which case the probe partial state is a perfect singlet with zero linear entropy: $S_L(\rho_{ab}) := 1 - \text{Tr}[\rho_{ab}^2] = 0$. This result does not depend on the accuracy of the perturbative estimate of J_{eff} , for we would obtain the same value provided that $J_{\text{eff}} > 0$ is temperature independent. On the other hand, the probes are also correlated (albeit weakly) with the bus, since the effective probe coupling is a result of perturbative admixture of virtual excited bus states in the ground-state manifold; the probe entanglement, even at zero temperature, is not complete.

This issue is clarified by computing the connected correlation between the probes under the adiabatic assumption and comparing it with (13) [obtained from the approximation, $J_{ab}(\beta) \approx J_{\text{eff}}$]. This is achieved by recasting the correlation [Eq. (8)] into a form involving the non-perturbative effective Hamiltonian $H_S = H'_b + H_p$. To this end, we make use of the canonical transformation [Eq. (2)] to get

$$\langle \tau_a \cdot \tau_b \rangle = \frac{\text{Tr} \left[e^{-\beta H_S} \left(e^{-i\hat{S}} \tau_a \cdot \tau_b e^{i\hat{S}} \right) \right]}{\text{Tr} \left[e^{-\beta H_S} \right]}. \quad (14)$$

From the adiabatic continuity assumption [Eqs. (3)-(4)],

we get

$$\langle \tau_a \cdot \tau_b \rangle = \frac{\text{Tr}_p \left[e^{-\beta H_p} \left(\text{Tr}_b e^{-\beta H_b} e^{-i\hat{S}} \tau_a \cdot \tau_b e^{i\hat{S}} \right) \right]}{\text{Tr}_p [e^{-\beta H_p}] \text{Tr}_b [e^{-\beta H_b}]} \quad (15)$$

$$= \frac{\text{Tr}_p \left[e^{-\beta H_p} \left\langle e^{-i\hat{S}} \tau_a \cdot \tau_b e^{i\hat{S}} \right\rangle_{\text{bus}} \right]}{\text{Tr}_p [e^{-\beta H_p}]} \quad (16)$$

It is clear that the canonical transformed Hamiltonian must be a scalar in the probe's operators, that is, $H_p \sim \tau_a \cdot \tau_b$, and hence with the same form as found in perturbation theory [$H_{\text{eff}} \sim \tau_a \cdot \tau_b$]. However, the operator being averaged with respect to the bus is not simply $\tau_a \cdot \tau_b$:

$$e^{-i\hat{S}} \tau_a \cdot \tau_b e^{i\hat{S}} := \tau_a^R \cdot \tau_b^R = \tau_a \cdot \tau_b - i \left[\hat{S}, \tau_a \cdot \tau_b \right] + \dots \quad (17)$$

Physical states constructed from the effective Hamiltonian (11) yield the correct averages for the ‘‘renormalized’’ spins (those in Fig. 2, right), but not for the original spins. Indeed, the spin operators must be renormalized if one wishes to get averages corresponding to real spin degrees of freedom. The second term in (17) gives an important correction to $\langle \tau_a \cdot \tau_b \rangle$ [Eq. (13)], inhibiting $\tau_{a(b)}$ partial states with zero linear entropy (in particular, perfect singlets).

Using symmetry alone, we can relate the scalar product involving real and renormalized spins. The formal derivation is done in Appendix 1 [see Eqs. (37)-(47)]; here it is sufficient to observe that if the robust gap situation is verified, taking averages with respect to the spin bus is tantamount to taking ground-state averages $\langle \dots \rangle_{\text{bus}} = \langle \psi_0 | \dots | \psi_0 \rangle$; the result is a probe-only operator that, by symmetry, has the form

$$\langle e^{-i\hat{S}} \tau_a \cdot \tau_b e^{i\hat{S}} \rangle_{\text{bus}} = \eta \mathbb{I}_{2 \otimes 2} + (1 - \Phi) \tau_a \cdot \tau_b, \quad (18)$$

with $\eta = \eta(\alpha)$ and $\Phi = \Phi(\alpha)$, real, bounded, and temperature independent. No other operators enter in this formula (18) because the canonical transformation \hat{S} will necessarily produce rotational-invariant probe operators (and there are just two in $2 \otimes 2$, namely, the identity and the scalar product). The parameters η and Φ , to which we refer as canonical corrections, describe how much the states $|\Psi_{0,s}\rangle$ and $|\Psi_{0,m}\rangle$ differ from the product states $|\psi_0\rangle \otimes |\chi^s\rangle$ and $|\psi_0\rangle \otimes |\chi_m^t\rangle$ [see Eqs. (3) and (4)].

The probes correlation is obtained by averaging the latter equation. It is instructive to consider the zero-temperature case,

$$\langle \tau_a \cdot \tau_b \rangle_{T=0} = \langle \Psi_{0,s} | \tau_a \cdot \tau_b | \Psi_{0,s} \rangle \quad (19)$$

$$= \langle \chi^s, \psi_0 | \tau_a^R \cdot \tau_b^R | \psi_0, \chi^s \rangle \quad (20)$$

$$= -3 + \eta + 3\Phi. \quad (21)$$

The last equality implies the restriction $4 \geq \eta + 3\Phi \geq 0$. The scenario of perfect entanglement, $E(\rho_{ab}) = 1$, requires $\eta + 3\Phi = 0$. Indeed, considering the approximation of Ref. [24] is equivalent to taking $\tau_{a(b)}^R \simeq \tau_{a(b)}$,

which results in quasiperfect AF correlations for $T = 0$: $\langle \tau_a \cdot \tau_b \rangle_{T=0} \simeq \langle \chi^s, \psi_0 | \tau_a \cdot \tau_b | \psi_0, \chi^s \rangle = -3$. This approximation is strictly valid when $\eta \simeq \Phi \simeq 0$. At finite temperatures, we must use the form of the probe Hamiltonian $H_p := (\Delta_{ab}/4) \tau_a \cdot \tau_b$, to obtain,

$$\langle \tau_a \cdot \tau_b \rangle = \eta + (1 - \Phi) \langle \tau_a \cdot \tau_b \rangle_{\text{can}}. \quad (22)$$

where,

$$\langle \tau_a \cdot \tau_b \rangle_{\text{can}} = \frac{\text{Tr}_p [e^{-\beta H_p} \tau_a \cdot \tau_b]}{\text{Tr}_p [e^{-\beta H_p}]} = \frac{e^{-\beta \Delta_{ab}} - 1}{e^{-\beta \Delta_{ab}} + 1/3}. \quad (23)$$

The parameter Δ_{ab} is, by definition, the singlet-triplet gap: $\Delta_{ab} = \langle \chi^t | H_p | \chi^t \rangle - \langle \chi^s | H_p | \chi^s \rangle$. By virtue of the transformation (3-4) this equals,

$$\Delta_{ab} = \langle \Psi_{0,m} | H | \Psi_{0,m} \rangle - \langle \Psi_{0,s} | H | \Psi_{0,s} \rangle. \quad (24)$$

Contrary to the real effective coupling, $J_{ab}(\beta)$, the coupling $\Delta_{ab}/4$ is effectively temperature independent.

Finally, we relate the real effective coupling defined by Eq. (7) with the canonical parameters. This is accomplished by equating the right-hand sides of Eqs. (8) and (22) and solving for $J_{ab}(\beta)$. We get,

$$J_{ab}(\beta) = \frac{1}{4\beta} \ln \left[\frac{3(\Phi - \eta) + (4 - 3\Phi - \eta) \exp(\beta \Delta_{ab})}{4 - \Phi + \eta + (\Phi + \eta/3) \exp(\beta \Delta_{ab})} \right]. \quad (25)$$

We thus have achieved a parametrization of the temperature dependence of ρ_{ab} as a function of three parameters, the singlet-triplet gap, Δ_{ab} , and the canonical corrections Φ and η :

$$\rho_{ab}(\beta) = \frac{\mathbb{I}_{ab}}{4} + \frac{1}{4} \left(\eta/3 + (1 - \Phi) \frac{e^{-\beta \Delta_{ab}} - 1}{3e^{-\beta \Delta_{ab}} + 1} \right) \tau_a \cdot \tau_b. \quad (26)$$

These parameters can in principle be computed in perturbation theory (see Appendix 2):

$$\Delta_{ab} \simeq (2J\alpha)^2 \tilde{\chi}_r(0), \quad (27)$$

$$\Phi \simeq (2J\alpha/\sqrt{3})^2 \sum_{m>0} \sum_{\mu=x,y,z} \frac{|\langle \psi_0 | \mathbf{S}_A^\mu - \mathbf{S}_B^\mu | \psi_m \rangle|^2}{(E_m - E_0)^2} \quad (28)$$

$$\eta = O(\alpha^4 J^4 / \Delta_0^4). \quad (29)$$

In Eq. (28), the states of the spin bus are denoted by $|\psi_m\rangle$ (with eigenenergy E_m). The canonical parameters for small α can be computed by diagonalizing the spin bus Hamiltonian, $H_0 |\psi_k\rangle = E_k |\psi_k\rangle$. This is, however, only possible in a few models whose analytical solutions are known, as in the case of the 1D XY model [25], or in situations where conformal symmetry fixes the form of dynamical correlations (e.g., critical spin chains) [24]. In general, whether the canonical parameters describe the correlations of the probes accurately for a given spin model must be investigated by comparing result (22) [or equivalently, (25)] with numerical simulations. We recall that this model will only describe the partial state

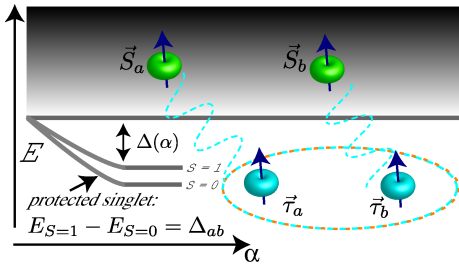


Figure 3: Schematic of the opening of a gap Δ_{ab} by two spin-1/2 probes that couple locally to a bus with arbitrary strength αJ . The low-energy sector is separated from excited states by the gap $\Delta(\alpha)$ and has a singlet-triplet separation, Δ_{ab} , which is enhanced with the dimensionality of the bus. If the singlet is localized near the probes, they will be highly entangled even at large distances (the so-called LDE). We show that Δ_{ab} is a robust gap in the square AF lattice (see text).

of probes interacting with large lattices if adiabatic continuity and a robust gap hold (Appendix 1). In what follows, we describe a class of systems that shows impressive agreement with this canonical theory.

III. Quantum Monte Carlo results

Our systems consist of 2D finite lattices \mathcal{L} , with $N = l \times n_c$ spins-1/2 and two extra probes, where l is the number of longitudinal sites and n_c stands for the number of coupled chains, varying from $n_c = 1$ (spin chain) to $n_c = l$ (square lattice) (see Fig. 1 for a possible geometry). The Hamiltonian of the lattice is

$$H_0 = J \sum_{\langle i,j \rangle} \vec{S}_i \cdot \vec{S}_j, \quad (30)$$

with $J > 0$. The qubit probes interact with the spins at the boundary of the most central chain through an isotropic interaction [Eq. (1)]. We expect a significant change in LDE from the common 1D scenario analyzed in [5, 16], as the physics of a 2D spin system is very distinct. In particular, the 2-leg ladder chain has an Haldane gap [26] which should play against a large J_{ab} ; very massive excitations, $\Delta_0 \simeq 0.504J$, make the correlations die particularly fast [27]. Our QMC simulations were performed with the library looper from the Algorithms and Libraries for Physics Simulations (ALPS) project [28] (see Appendix 3 for details on the numerics).

A. Thermal LDE

We now outline the main results from the QMC simulations for the entire family of AF lattices. Among the 20 spin systems studied, only the spin chain ($n_c = 1$)

was addressed in previous works. This system is able to generate a large amount of LDE in the weak coupling regime, in accordance with the numerical result from [5]; our choice of coupling entails, for $l = 20$ and $n_c = 1$, $J_p^2/\Delta_0 \simeq 0.015J$ (with Δ_0 extracted from [27])—well inside perturbation limits. The numerical results indeed show probes almost maximally entangled. Table I below summarizes the results for the two most representative lattices.

gaps	Δ_0/J	Δ_{ab}/J
<i>spin chain</i>	$3.2/l \simeq 0.16$	5.07×10^{-4}
<i>square lattice</i>	$9.26/l^2 \simeq 0.02$	3.04×10^{-3}
canonical corrections	Φ	η
<i>spin chain</i>	1.03×10^{-2}	6.27×10^{-4}
<i>square lattice</i>	1.46×10^{-1}	-1.37×10^{-2}

Table I: The singlet-triplet gap Δ_{ab} and canonical parameters in representative systems for $\alpha = 0.05$. The canonical parameters are calculated by fitting the QMC data for different temperatures with Eq. (22). The expressions for $\Delta_0 \equiv \Delta_{ab}(\alpha = 0)$ were taken from Refs. [27] and [29].

These results show a curious property of the 2D spin system: Whereas for $n_c = 1$, the spin-triplet gap due to the probes is $\Delta_{ab} \simeq 3 \times 10^{-3}\Delta_0$, for $n_c = 20$, this gap is $\Delta_{ab} \simeq 1.3 \times 10^{-1}\Delta_0$, a difference of about 2 orders of magnitude for the ratio Δ_{ab}/Δ_0 . This leads to a much more robust LDE against temperature in 2D, albeit at the cost of a larger canonical correction, $\Phi \sim 0.15$, suppressing the possibility of $E_C \simeq 1$ at $T = 0$. Indeed, taking the values for Φ and η in table I and using Eqs. (21) and (9), we get, at $T = 0$, $E_C \simeq 0.984$ for the spin chain and $E_C \simeq 0.788$ for the square lattice. A clear picture of LDE is now given in light of the exposition of the previous section: The singlet is strongly localized at the boundary sites (the probes) for $n_c = 1$, and thus the mechanism for LDE is quasi optimal, making the effective Hamiltonian picture [Eq. (11)] extremely accurate. This is not the case in general, where the renormalization of spins [Eq. (17)] cannot be ignored, a fact particularly evident for the square lattice where $\Phi \sim O(10^{-1})$.

Let us investigate these issues more carefully. We postpone the implication of these results to the emergence of “robust gaps” in 2D. We focus first on the small probe-bus coupling, $\alpha = 0.05$, before venturing away from perturbation theory. Figure 4 shows J_{ab} (for $k_B T = 2 \times 10^{-3}J$) and the entanglement “critical temperature” T_c . The scale of T_c is Δ_{ab} apart from small corrections (see Fig. 5, bottom panel). These plots show a clear enhancement of the ability of the antiferromagnet to generate long-range effective interactions among distant probes as one reaches the square lattice at thermal energies $k_B T = 2 \times 10^{-3}J$. The consequences for LDE are evident: The 2D lattices, with $n_c > 4$, mediate more entanglement at high temperatures (see later). In Fig. 4, a wiggly behavior up to

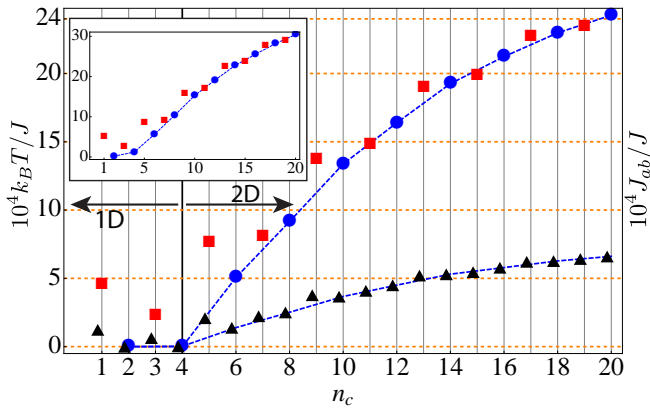


Figure 4: Black triangles show effective coupling, J_{ab} , at a distance $l = 20$, as a function of n_c , number of transverse chains ($k_B T = 2 \times 10^{-3} J$). Blue dots (n_c even) and red squares (n_c odd) show temperature above which LDE vanishes. The inset shows canonical coupling (i.e., the probe’s singlet protection gap of Fig. 3) in the same units used to represent J_{ab} . The error bars from QMC cannot be seen as they are typically below 1%; $\alpha = 0.05$ in all plots.

$n_c = 4$ and a transition for $n_c > 4$ are also observed; that is, the increase of Δ_{ab} (and also J_{ab}) becomes smooth because the Haldane gap, very large for $n_c = \{2, 4\}$ [27], gets suppressed.

We would expect the ground state of 2D antiferromagnets to reduce substantially the LDE because of the symmetry breaking at $T = 0$, for large lattices [17, 29, 30]; the finite sub-lattice magnetization should reduce the amount of genuine quantum correlations shared by the probes. This is borne out by the results of the QMC simulations, shown in Fig. 6, where J_{ab} (and hence entanglement) is found to decrease at low temperatures, $k_B T \lesssim 10^{-4} J$, when the number of chains increases. Nevertheless, at higher temperatures, the opposite occurs: J_{ab} increases with n_c ; this reflects the increase of the probe’s protection gap, Δ_{ab} , for it sets the temperature scale at which entanglement vanishes.

In Fig. 6, the lines are near perfect fits to the Monte Carlo data, using Eq. (25). For sake of clarity, we have presented the agreement just for four lattices, although all fits show the same degree of accuracy. The observed linear dependence of J_{ab} with the temperature for $T \rightarrow 0$ is easily understood: A zero-temperature (finite) entanglement below the maximum value of 1 requires $\beta J_{ab}(\beta) \rightarrow \text{constant}$, when $\beta \rightarrow \infty$. This constant can be derived from Eq. (25), yielding,

$$\beta J_{ab}(\beta) \xrightarrow{\beta \rightarrow \infty} \frac{1}{4} \ln \left[\frac{4 - 3\Phi - \eta}{\Phi + \eta/3} \right]. \quad (31)$$

Thus, the canonical corrections (Φ and η) determine the low-temperature physics of the probes. It is instructive to notice that one recovers the condition from quasi-perfect

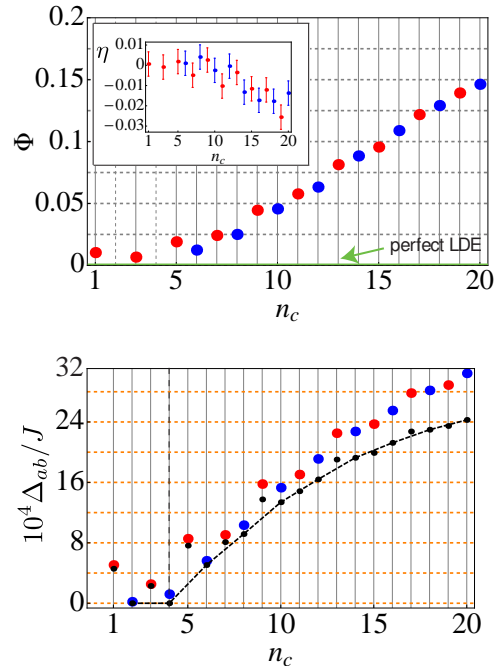


Figure 5: (top) Canonical correction Φ for the same family of spin lattices of Fig. 4. The inset shows that the η correction is negligible compared to Φ ; the bars represent an estimate of the error due to QMC fluctuations. The $n_c = 2$ and $n_c = 4$ systems are not represented since the data do not provide reliable values for canonical corrections. (bottom) The singlet protection gap for finite probe coupling ($\alpha = 0.05$) in blue (n_c even) and red dots (n_c odd). The critical temperature is represented (small black dots) for comparison.

LDE derived earlier [Eq. (21)]; $\beta J_{ab} \rightarrow \infty$ as $3\Phi + \eta \rightarrow 0$ and thus, according to Eq. (8), $\langle \tau_a \cdot \tau_b \rangle_{T=0} \simeq -3$. This is a very special scenario occurring in 1D antiferromagnets and also in dimerized chains [25]. The present results reveal that quasiperfect LDE is also mediated by the three-ladder chain, $3\Phi + \eta \simeq 0.007$. As soon as we approach the 2D scenario, more precisely when $n_c > 4$, the Φ correction gets larger (see Fig. 5 for the variation of Φ with n_c) and a fraction of the entanglement is lost.

In our simulations, the value of η is negligible (a careful inspection shows that the fits we present are virtually indistinguishable from the fits with $\eta = 0$ up to $\alpha \simeq 0.1$), and the $n_c = 3$ spin system mediates the largest amount of LDE at $T = 0$ (see Fig. 5), $E_C \simeq 0.997$. Curiously, this behavior is not altered by varying the coupling in the entire range we have simulated: $\alpha \in [0.05, 0.2]$. In fact, for large α , namely, $\alpha = 0.2$, the discrepancy between the $n_c = 1$ and $n_c = 3$ lattices is quite significant: $\Phi \simeq 0.238$ against $\Phi \simeq 0.079$. This is a very interesting property of the three-leg ladder: the ability of generating high-quality ground-state entanglement for a wide range of probe-bus coupling.

For the highest temperatures simulated, the effective

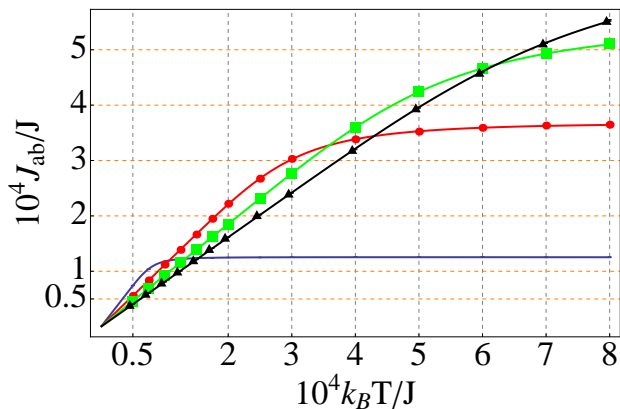


Figure 6: The points in the plot show J_{ab} as function of the temperature from QMC simulations for $\alpha = 0.05$. The lines stand for the fit with the expression given in Eq. (25), with $n_c = 1$ (blue), $n_c = 10$ (red; circles), $n_c = 15$ (green; squares), and $n_c = 20$ (black; triangles). The agreement between the QMC data is excellent, resulting in an average deviation of $\sim 0.1 - 1\%$, depending on the lattice.

coupling saturates (Fig. 6) to a constant value, $\Delta_{ab}(1 - \Phi)/4$, when η is negligible (i.e., not far away from the perturbation limit, $\alpha \lesssim 0.1$), suffering a slight change with temperature otherwise,

$$J_{ab}(T) \simeq \frac{\Delta_{ab}}{4} (1 - \Phi) - \frac{k_B T}{12} \eta + O\left(\frac{\Delta_{ab}^2 \Phi}{k_B T}\right). \quad (32)$$

An estimate of the entanglement critical temperature, T_c , is obtained by noting that $J_{ab}(T)$ has already saturated when the concurrence vanishes. Indeed, combining Eqs. (10) and (32), we obtain,

$$k_B T_c \simeq 0.93 \Delta_{ab} (1 - \Phi). \quad (33)$$

This agrees with the numerical results within 1%; in Fig. 5 (bottom), the increasing mismatch between $k_B T_c$ and the gap Δ_{ab} with n_c reflects the increase in Φ . This equation for T_c generalizes the previous result for the spin-1/2 AF Heisenberg ring [24]—where Δ_{ab} is equal to $4\alpha^2 \tilde{\chi}_r(0)$ in the perturbative regime [Eq. (27)]—by the inclusion of the Φ correction.

The square lattice is the system with the best thermal LDE robustness, despite its appreciable reduction of zero temperature entanglement, $\Phi \simeq 0.146$, a fact explained by the emergence of a large singlet-triplet gap, Δ_{ab} , which is about 6 times the protection gap of the single spin chain. The regime of high temperatures, $k_B T \gtrsim \Delta_0$, is not described by Eq. (25) anymore, which assumes negligible thermal occupancy of excited states of the spin bus, a crucial assumption of our analytical modeling. However, according to our estimate [Eq. (33)], no LDE is expected in this temperature range, because it vanishes at much lower temperatures; $J_{ab}(\beta)$ should decrease with

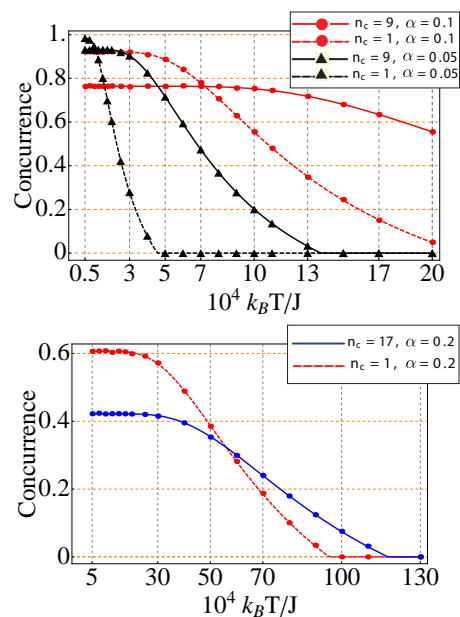


Figure 7: Concurrence, an entanglement monotone for qubits, as a function of temperature for different lattices and couplings. Lattices supporting more entanglement at strictly $T = 0$ have worse performance at higher temperatures. The lines are fits using Eq. (25) for $J_{ab}(\beta)$ and Eqs. (8) and (9). The fits are nearly perfect for the entire temperature range in which entanglement persists.

the temperature at some point and eventually drop to zero, reflecting totally uncorrelated probes. The initial drop of J_{ab} with T is captured by Eq. (32).

B. Beyond weak coupling

Figures 4 and 5 deal with relatively small probe-bus coupling, but the results presented so far are more general. For instance, choosing a sufficiently large α to strongly suppress the zero-temperature entanglement via partial frustration among the neighborhood of the bulk spins connected with the probes, we again find excellent agreement with Eq. (25). For intermediate probe-bus coupling, $\alpha = 0.1$ and $\alpha = 0.2$, the measured concurrence is fitted with an expression derived from Eq. (22), as shown in Fig. 7. These results show that in all our measured systems, the conditions for our model hold, namely, a singlet-triplet low-energy sector and an excited bus sector which is not significantly populated. This is surprising, particularly in the case of large lattices, which have a gap Δ_0 smaller than αJ ; not only do we find a well protected singlet with a considerable amount of LDE, but the lowest singlet and triplet remain separated from the rest of the spectrum, allowing a complete description of entanglement only in terms of these two energy levels.

On the other hand, though the strong coupling to the

spin bus reduces the zero temperature entanglement, it also allows a larger split between the singlet and triplet, leading to entangled probes at much higher temperatures. Typically, exchange interactions in antiferromagnets can be of the order of 0.1 eV, resulting in an effective coupling of the order of 0.3 meV for the square lattice ($l = 20$) at temperature ~ 12 K and $\alpha = 0.2$. This is to be compared with the value of 0.01 – 0.1 meV achievable in quantum dot spins [31], although decoherence effects in spin lattices can lessen this difference. The critical temperature (above which the correlations shared by the probes are completely classical) can be increased by a factor of 20 from a weakly coupled spin chain ($\alpha = 0.05$) to an intermediate coupled ($\alpha = 0.2$) 2D lattice, entanglement surviving up to $k_B T \simeq 1.2 \times 10^{-2} J$ (Fig. 7)—an appreciable enhancement of the thermal robustness of such correlations.

C. Robust gaps in 2D

The QMC results analyzed in light of our model show that two probes interacting with AF spin systems open a gap Δ_{ab} which is enhanced with the dimensionality of the system. For the square lattice and probe-bus coupling $J_p = 0.05J$, the gap reads $\Delta_{ab} \simeq 3.04 \times 10^{-3} J$, a *robust gap*. The point is that the 20×20 lattice, without probes, has a small singlet-triplet gap $\Delta_0 \simeq 0.02J$ (see Refs. [29, 30]), making the bus-probe interaction non-perturbative. Even so, these probes opened a considerable gap, and their reduced state displays a large amount of $T = 0$ entanglement, $E_C \simeq 0.79$, in resemblance to the spin chain bus with probes. The situation in the 2D lattice is very distinct, though, because for the spin chain, $\Delta_{ab}/\Delta_0 = O(10^{-3})$, whereas in the square lattice, this ratio is 2 orders of magnitude greater, $\Delta_{ab}/\Delta_0 = O(10^{-1})$.

The whole analysis of this article follows from fits of the probe-probe correlation $\langle \tau_a \cdot \tau_b \rangle$ computed by QMC for several temperatures to a simple analytical model derived under adiabatic continuity hypothesis. These fits provide the values of Δ_{ab} and the canonical corrections (Φ and η). Our reliance on this model is not exclusively due to the nearly perfect fits to which it leads (see Fig. 8).

A crucial test of this model is given by checking the scaling of Φ and η with α [Eqs. (28) and (29)]. We give an estimate for this scaling for the spin chain with $L = 20$ based on three simulations in Fig. 9: The dependence of Φ and η with α can be read from the slopes; $\Phi \sim \alpha^{2.26}$ and $\eta \sim \alpha^{3.95}$, which agrees well with the theoretical prediction for weak coupling given by our model ($\Phi \sim \alpha^2$ and $\eta \sim \alpha^4$). Recall that for $\alpha = 0.2$, we have $\alpha J > \Delta_0$, and thus the system is already well inside the intermediate coupling regime. Nevertheless, the fits are very good up this value of coupling (see Fig. 7)—we again emphasize that this is particularly remarkable for the 2D sys-

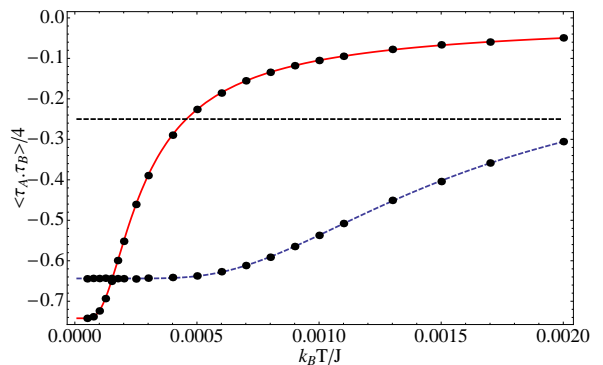


Figure 8: Probe-probe correlation, $\langle \tau_a \cdot \tau_b \rangle / 4$, at a distance $l = 20$, as a function of temperature for the spin chain (red) and the square lattice (blue); $\alpha = 0.05$ in both plots. The black dots are given by the QMC simulations (the error bars from QMC cannot be seen as they are typically below 1%). The lines stand for the fit with Eq. (22). The dashed line separates classical correlations (above) from quantum correlations (below). The red curve shows that the quality of the fits extends beyond the region where entanglement is nonzero.

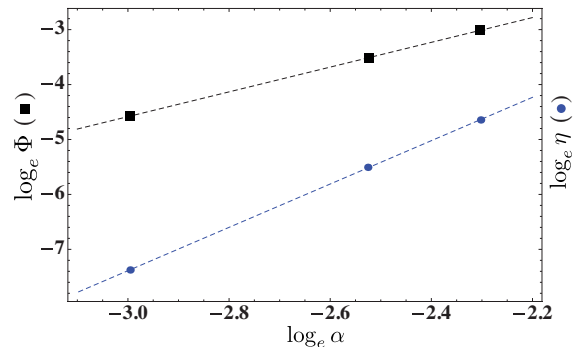


Figure 9: Log-log representation (dots) of $\Phi(\alpha)$ and $\eta(\alpha)$ for a spin chain with $L = 20$ plus two probes—the $n_c = 1$ system of the article—and the respective linear fits (dashed lines).

tem, which is gapless in the thermodynamic limit and has a broken symmetry phase. These facts provide added confirmation of our analytical model and the conclusions drawn about the spectrum of the system and the emergence of robust gaps.

If states other than the lowest singlet and triplet contributed significantly to the spin correlations at the temperatures in which we still find entanglement, the quality of the fits, added to the fact that $\eta \ll \Phi$, would be an amazing coincidence indeed. Exact numerical diagonalizations could provide direct evidence of the spectrum, but these are very hard to perform for large 2D systems. We have used the algorithm `sparsediag` from ALPS to compute the three lowest energies for relatively small systems; Fig. 10 shows the emergence of robust gaps for two different lattices (4×3 and 6×3).

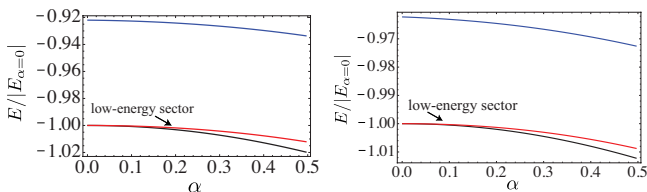


Figure 10: Plot of the low-energy spectrum for two different systems with 100 values of α in the range $[0, 0.5]$. The energy is scaled to the absolute value of the ground-state energy for $\alpha = 0$: (left) a lattice with $l = 4$ and $n_c = 3$ with gap $\Delta_0 = 0.52J$ and (right) a lattice with $l = 6$ and $n_c = 3$ with gap $\Delta_0 = 0.39J$. The crossover between weak and strong probe-bus coupling can be observed with the respective emergence of robust gaps.

IV. Conclusions

We observed an enhancement of LDE by varying the geometry of the magnetic spin systems serving as a quantum bus. We presented the first *direct* measurement of the probe correlation for finite temperature by means of QMC simulations with the ALPS algorithm. Also, we derived an analytical expression for the probe density matrix that completely describes the probe-probe entanglement for the systems we studied, even away from the weak-coupling regime. The importance of the dimensionality of the bus is twofold: On one hand, ground-state entanglement is reduced as we go from a 1D to a 2D bus; on the other hand, robustness of thermal entanglement increases considerably in the 2D, raising the possibility of entangling distant spin probes at temperatures as high as $T \simeq 1.2 \times 10^{-2} J/k_B$, where J is the nearest neighbor exchange constant of the bus, an appealing situation for quantum computation based on magnetic spins. Finally, we reported on a spin system supporting quasiperfect ground-state LDE more efficiently than the AF spin chain, particularly in the intermediate probe-bus coupling regime: the three-leg ladder chain.

We acknowledge the ALPS project [28] and the library `looper` that made possible the QMC simulations of the present article, and we also acknowledge the support of EU and FCT through POCI 2010 and PRAXIS Grant No. SFRH/BD/18292/04 (A.F.) and Grant No. SFRH/BPD/27160/2006 (J.V.L.).

Appendix 1

Full rotational symmetry entails that the probe density matrix can be written as function of a single $2 \otimes 2$ invariant,

$$\hat{\rho}_{ab} = \frac{1}{3e^{-\beta J_{ab}(\beta)} + e^{3J_{ab}(\beta)}} \exp(-\beta J_{ab}(\beta) \boldsymbol{\tau}_a \cdot \boldsymbol{\tau}_b), \quad (34)$$

This allows to parametrize the correlations between probes as

$$\langle \boldsymbol{\tau}_a \cdot \boldsymbol{\tau}_b \rangle = \frac{e^{-4\beta J_{ab}(\beta)} - 1}{e^{-4\beta J_{ab}(\beta)} + 1/3}. \quad (35)$$

This tells us very little for the moment since the temperature dependence of $J_{ab}(\beta)$ is unknown. On the other hand, by definition,

$$\langle \boldsymbol{\tau}_a \cdot \boldsymbol{\tau}_b \rangle = \frac{\text{Tr} [e^{-\beta H} \boldsymbol{\tau}_a \cdot \boldsymbol{\tau}_b]}{\text{Tr} [e^{-\beta H}]}, \quad (36)$$

and, using the canonical transformation \hat{S} ,

$$\langle \boldsymbol{\tau}_a \cdot \boldsymbol{\tau}_b \rangle = \frac{\text{Tr} [e^{-\beta H_S} e^{-i\hat{S}} \boldsymbol{\tau}_a \cdot \boldsymbol{\tau}_b e^{i\hat{S}}]}{\text{Tr} [e^{-\beta H_S}]}. \quad (37)$$

The transformed Hamiltonian is $H_S = H_p + H'_b$; the corresponding eigenbasis is made of product states [Eqs. (3)-(4)]. Under the assumption that $k_B T \ll \Delta(\alpha)$ (i.e., that the temperature is much smaller than the gap to excited states of the bus), we can limit the trace to the states of the form $|\psi_0\rangle \otimes |\chi\rangle$, where $|\chi\rangle$ is any probe state and $|\psi_0\rangle$ is the nondegenerate ground state of the spin bus. This leads to

$$\langle \boldsymbol{\tau}_a \cdot \boldsymbol{\tau}_b \rangle = \frac{\text{Tr}_p [e^{-\beta H_p} \langle \psi_0 | e^{-i\hat{S}} \boldsymbol{\tau}_a \cdot \boldsymbol{\tau}_b e^{i\hat{S}} | \psi_0 \rangle]}{\text{Tr}_p [e^{-\beta H_p}]}, \quad (38)$$

where $\text{Tr}_p(\dots)$ is a trace over probe states only. Since the operator $\boldsymbol{\tau}_a \cdot \boldsymbol{\tau}_b$ is diagonal in bus space, this can obviously be written as

$$\langle \boldsymbol{\tau}_a \cdot \boldsymbol{\tau}_b \rangle = \frac{1}{\text{Tr}_p [e^{-\beta H_p}]} \text{Tr}_p \left[e^{-\beta H_p} \sum_m \langle \psi_0 | e^{-i\hat{S}} | \psi_m \rangle \boldsymbol{\tau}_a \cdot \boldsymbol{\tau}_b \langle \psi_m | e^{i\hat{S}} | \psi_0 \rangle \right] \quad (39)$$

$$= \frac{\text{Tr}_p [e^{-\beta H_p} \sum_m A_m \boldsymbol{\tau}_a \cdot \boldsymbol{\tau}_b A_m^\dagger]}{\text{Tr}_p [e^{-\beta H_p}]}, \quad (40)$$

where $A_m \equiv \langle \psi_0 | e^{-i\hat{S}} | \psi_m \rangle$ is an operator defined in probe space. By symmetry, the operator

$$\sum_m A_m \boldsymbol{\tau}_a \cdot \boldsymbol{\tau}_b A_m^\dagger = \langle \psi_0 | e^{-i\hat{S}} \boldsymbol{\tau}_a \cdot \boldsymbol{\tau}_b e^{i\hat{S}} | \psi_0 \rangle \quad (41)$$

must be a scalar in probe space and therefore of the form

$$\sum_m A_m \boldsymbol{\tau}_a \cdot \boldsymbol{\tau}_b A_m^\dagger = \eta + (1 - \Phi) \boldsymbol{\tau}_a \cdot \boldsymbol{\tau}_b, \quad (42)$$

where η and Φ are, by construction, temperature-independent renormalization constants. Since $\text{Tr}_p [\boldsymbol{\tau}_a \cdot \boldsymbol{\tau}_b] = 0$, and

$$(\boldsymbol{\tau}_a \cdot \boldsymbol{\tau}_b)^2 = 3 - 2\boldsymbol{\tau}_a \cdot \boldsymbol{\tau}_b, \quad (43)$$

we obtain

$$\mathrm{Tr}_p \left[\sum_m A_m \tau_a \cdot \tau_b A_m^\dagger \right] = 4\eta, \quad (44)$$

$$\mathrm{Tr}_p \left[\sum_m \tau_a \cdot \tau_b A_m \tau_a \cdot \tau_b A_m^\dagger \right] = 12(1 - \Phi). \quad (45)$$

With these definitions it is clear that

$$\langle \tau_a \cdot \tau_b \rangle = \eta + (1 - \Phi) \langle \tau_a \cdot \tau_b \rangle_{\mathrm{can}}, \quad (46)$$

where,

$$\langle \tau_a \cdot \tau_b \rangle_{\mathrm{can}} := \frac{\mathrm{Tr}_p [e^{-\beta H_p} \tau_a \cdot \tau_b]}{\mathrm{Tr}_p [e^{-\beta H_p}]} = \frac{e^{-\beta \Delta_{ab}} - 1}{e^{-\beta \Delta_{ab}} + 1/3}. \quad (47)$$

This looks exactly like the preceding expression, except that now Δ_{ab} , unlike J_{ab} , is temperature independent. So we achieve a parametrization of $\langle \tau_a \cdot \tau_b \rangle$ in terms of three temperature-independent parameters Δ_{ab} , Φ , and η . This result, although simple, has important consequences; for instance, we see that symmetry implies that Δ_{ab} is in fact the gap separating the probe's singlet and the probe's triplet up to any order. We can thus write,

$$\Delta_{ab} = E_{\mathrm{triplet}}(\alpha) - E_{\mathrm{singlet}}(\alpha). \quad (48)$$

Using equations (35), (46) and (47), we can express $J_{ab}(\beta)$ explicitly in these temperature-independent parameters:

$$J_{ab}(\beta) = \frac{1}{4\beta} \ln \left[\frac{3(\Phi - \eta) + (4 - 3\Phi - \eta) \exp(\beta \Delta_{ab})}{4 - \Phi + \eta + (\Phi + \eta/3) \exp(\beta \Delta_{ab})} \right]. \quad (49)$$

In Appendix 2 we derive the expression for Φ , and show that it is of second order in the small parameter $J\alpha/\Delta$.

Appendix 2

We now compute the canonical corrections, Φ and η , to the probe canonical correlation [Eq. (47)] in perturbation theory. We assume the following conditions to hold: (1) the temperature is small enough not to generate real excitations of the spin lattice system and (2) the probes couple weakly to the spin bus via an isotropic interaction with strength αJ , such that $\alpha J \ll \Delta_0$. In this limit, we can use the Schrieffer-Wolff prescription for the canonical generator \hat{S} [32],

$$V + i [H_0, \hat{S}] = 0,$$

where H_0 is the bus Hamiltonian and V the bus-probe coupling. The canonical generator \hat{S} has nonzero matrix elements only between the ground state manifold (at zero coupling) and excited states of order $\sim \mathcal{O}(\alpha J/\Delta_0)$. The transformed Hamiltonian is, to second order in V ,

$$H_S := H_0 - \frac{i}{2} [\hat{S}, V].$$

To calculate the probe correlation, we expand the renormalized spin operators in powers of \hat{S} :

$$\begin{aligned} \langle \tau_a \cdot \tau_b \rangle &= \mathrm{Tr} \left[e^{-i\hat{S}} \rho_{ab} e^{i\hat{S}} e^{-i\hat{S}} \tau_a \cdot \tau_b e^{i\hat{S}} \right] \quad (50) \\ &= \mathrm{Tr} \left[\frac{e^{-\beta H_S}}{\mathcal{Z}} \left(\tau_a \cdot \tau_b - i [\hat{S}, \tau_a \cdot \tau_b] \right. \right. \\ &\quad \left. \left. - \frac{1}{2} [\hat{S}, [\hat{S}, \tau_a \cdot \tau_b]] + O\left(\frac{J^3 \alpha^3}{\Delta_0^3}\right) \right) \right], \quad (51) \end{aligned}$$

with $\mathcal{Z} := \mathrm{Tr} [\exp(-\beta H_S)]$. From the latter result, we can express the \hat{S} -renormalized spins as a function of the original spins:

$$\tau_a \cdot \tau_b \xrightarrow{\hat{S}} \tau_a^R \cdot \tau_b^R = \tau_a \cdot \tau_b + \xi_{ab}, \quad (52)$$

with,

$$\xi_{ab} = -\frac{1}{2} [\hat{S}, [\hat{S}, \tau_a \cdot \tau_b]] + O(J^3 \alpha^3 \Delta_0^{-3}), \quad (53)$$

implying that the ground state of the probes ρ_{ab} will never be a perfect singlet if $\langle \xi_{ab} \rangle_\beta$ is nonnegligible. The trace in Eq. (51) can be performed in two steps: (1) tracing out the bus by considering just the overlap with the ground-state, which is justified by the low-temperature condition, and (2) performing a thermal average in the $2 \otimes 2$ Hilbert space of the probes.

The first-order term does not contribute as the generator \hat{S} has null matrix elements in the ground state,

$$\langle \psi_0 | [\hat{S}, \tau_a \cdot \tau_b] | \psi_0 \rangle = [\langle \psi_0 | \hat{S} | \psi_0 \rangle, \tau_a \cdot \tau_b] = 0. \quad (54)$$

Then we are left with a zero-order term,

$$C_0 = \mathrm{Tr} \left[\frac{e^{-\beta H_S}}{\mathcal{Z}} \tau_a \cdot \tau_b \right],$$

yielding the canonical correlation, $\langle \tau_a \cdot \tau_b \rangle_{\mathrm{can}}$, and with a second-order correction C_2 ,

$$C_2 = -\frac{1}{2\mathcal{Z}} \mathrm{Tr} \left\{ e^{-\beta H_S} [\hat{S}, [\hat{S}, \tau_a \cdot \tau_b]] \right\}. \quad (55)$$

We must have some care to evaluate the preceding thermal average. Let us reproduce the main steps,

$$\begin{aligned} C_2 &= -\frac{1}{2\mathcal{Z}} \mathrm{Tr} \left[e^{-\beta H_S} \left(\hat{S} \hat{S} \tau_a \cdot \tau_b \right. \right. \\ &\quad \left. \left. - 2\hat{S} \tau_a \cdot \tau_b \hat{S} + \tau_a \cdot \tau_b \hat{S} \hat{S} \right) \right] \quad (56) \\ &\simeq -\frac{1}{\mathcal{Z}} \sum_{k \geq 0} \mathrm{Tr}_{a,b} \left[\langle \psi_0 | e^{-\beta H_S} | \psi_k \rangle \right. \\ &\quad \left. \langle \psi_k | \left(\hat{S} \hat{S} \tau_a \cdot \tau_b - \hat{S} \tau_a \cdot \tau_b \hat{S} \right) | \psi_0 \rangle \right]. \quad (57) \end{aligned}$$

The effective Hamiltonian has no matrix elements between eigenstates belonging to different sectors (up to

the order at which we are working), which simplifies the above summation as only the ground-state contributes [compare with Eqs. (37)-(38)]:

$$\langle \psi_0 | e^{-\beta H_S} | \psi_k \rangle = e^{-\beta H_P} \langle \psi_0 | e^{-\beta H'_b} | \psi_k \rangle \delta_{0k}. \quad (58)$$

Indeed,

$$C_2 = -\frac{1}{Z} \text{Tr}_{a,b} \left\{ e^{-\beta H_P} \langle \psi_0 | \left(\hat{S} \hat{S} \boldsymbol{\tau}_a \cdot \boldsymbol{\tau}_b - \hat{S} \boldsymbol{\tau}_a \cdot \boldsymbol{\tau}_b \hat{S} \right) | \psi_0 \rangle \right\} \quad (59)$$

The averages of the quadratic terms $\sim \hat{S} \hat{S}$ must be done separately as \hat{S} does not commute with the probe operators in general. It is convenient to introduce the matrix elements,

$$\begin{aligned} S_{ab}(m, n) &:= \langle \psi_m | \hat{S} | \psi_n \rangle \\ &= \langle \psi_m | \mathcal{P}_m \hat{S} \mathcal{P}_n | \psi_n \rangle. \end{aligned} \quad (60)$$

In second-order perturbation theory, the generator reads [32],

$$\begin{aligned} S_{ab}(m, n) &= \frac{J\alpha \langle \psi_m | (\boldsymbol{\tau}_a \cdot \mathbf{S}_A + \boldsymbol{\tau}_b \cdot \mathbf{S}_B) | \psi_n \rangle}{i(E_m - E_n)} \\ &= \frac{J\alpha}{i\Delta_{mn}} (\boldsymbol{\tau}_a \cdot \langle \psi_m | \mathbf{S}_A | \psi_n \rangle \\ &\quad + \boldsymbol{\tau}_b \cdot \langle \psi_m | \mathbf{S}_B | \psi_n \rangle). \end{aligned} \quad (61)$$

Inserting the resolution of the identity $\sum_m |\psi_m\rangle\langle\psi_m|$ in the expression for C_2 , we get after some algebra,

$$C_2 = -\frac{4\alpha^2 J^2}{3} \sum_{k>0} \sum_{\mu=x,y,z} \frac{|\langle \psi_0 | (\mathbf{S}_A^\mu - \mathbf{S}_B^\mu) | \psi_k \rangle|^2}{\Delta_{k0}^2} \langle \boldsymbol{\tau}_a \cdot \boldsymbol{\tau}_b \rangle_{\text{can}}. \quad (62)$$

Indeed, we arrive at the desired result

$$\langle \boldsymbol{\tau}_a \cdot \boldsymbol{\tau}_b \rangle = \langle \boldsymbol{\tau}_a \cdot \boldsymbol{\tau}_b \rangle_{\text{can}} (1 - \Phi) + \eta, \quad (63)$$

$$\begin{aligned} \Phi &= \left(\frac{2\alpha J}{\sqrt{3}} \right)^2 \sum_{k>0} \sum_{\mu=x,y,z} \frac{|\langle \psi_0 | (\mathbf{S}_A^\mu - \mathbf{S}_B^\mu) | \psi_k \rangle|^2}{\Delta_{k0}^2} + \\ &\quad + O(\alpha^3), \end{aligned} \quad (64)$$

with $\langle \boldsymbol{\tau}_a \cdot \boldsymbol{\tau}_b \rangle_{\text{can}}$ given previously in Eqs. (46)-(47), and where $\eta = 0$ up to second-order perturbation theory since no constant term has emerged from our expansion. It can be shown that this term is at most of fourth order, $O[(J\alpha/\Delta)^4]$ [33].

Appendix 3

We have performed several careful checks of the results obtained from the ALPS code. Our looper simulations used the following Monte Carlo input parameters: number of thermalization steps, 15000, number of sweeps, 400000. As a check, we used larger values of these parameters with no change in the results. We have no evidence whatsoever that our simulations failed to converge.

An important check of convergence is obtained through the measurement of the staggered magnetization. In our simulation (for the square lattice and $\alpha = 0.05$), we obtained

$$\sqrt{\langle (M_s^z)^2 \rangle} = 0.18008, \quad (65)$$

which gives a value $\sqrt{3} \sqrt{\langle (M_s^z)^2 \rangle} \approx 0.31191$ close to the known value of the sub-lattice magnetization in the thermodynamic limit (our system is finite and has open boundary conditions which may explain the small deviation).

The QMC error bars for the correlations are typically below 1%; for instance, for the square lattice, $\alpha = 0.05$, and the lowest simulated temperature, we have an estimate from the simulations error $\{\boldsymbol{\tau}_a \cdot \boldsymbol{\tau}_b / 4\} \simeq 3 [\text{error_MQ} \{ \langle \tau_a^z \tau_b^z \rangle / 4 \}] = 0.000735$, while the value of the correlation in this case is $\langle \boldsymbol{\tau}_a \cdot \boldsymbol{\tau}_b \rangle / 4 = -0.214852$.

-
- [1] D. P. DiVincenzo, *Fortschritte der Physik* **48**, 771 (2000).
 - [2] J. I. Cirac and P. Zoller, *Phys. Rev. Lett.* **74**, 4091 (1995).
 - [3] D. P. DiVincenzo *et al.*, *Nature (London)* **408**, 339 (2000).
 - [4] X. Zhou *et al.*, *Phys. Rev. Lett.* **89**, 197903 (2002); S. C. Benjamin and S. Bose, *Phys. Rev. Lett.* **90**, 247901 (2003); Man-Hong Yung, S. C. Benjamin and S. Bose, *Phys. Rev. Lett.* **96**, 220501 (2006); Mark Friesen *et al.*, *Phys. Rev. Lett.* **98**, 230503 (2007).
 - [5] L. Campos Venuti, C. Degli Esposti Boschi, and M. Roncaglia, *Phys. Rev. Lett.* **96**, 247206 (2006).
 - [6] T. J. Osborne and M. A. Nielsen, *Phys. Rev. A* **66**, 032110 (2002).
 - [7] T. Zell, F. Queisser, and R. Klesse, *Phys. Rev. Lett.* **102**, 160501 (2009).
 - [8] G. D. Chiara, C. Brukner, R. Fazio, G. M. Palma and V. Vedral, *New. J. Phys.* **8**, 95 (2006).
 - [9] W. H. Zureck, *Rev. Mod. Phys.* **75**, 715 (2003).
 - [10] D. Braun, *Phys. Rev. Lett.* **89**, 277901 (2002).
 - [11] F. Bennatti, R. Floreanini, and M. Piani, *Phys. Rev. Lett.* **91**, 070402 (2003).
 - [12] J. P. Paz and A. J. Roncaglia, *Phys. Rev. Lett.* **100**, 220401 (2008).
 - [13] S. Oh and J. Kim, *Phys. Rev. A* **73**, 062306 (2006).
 - [14] D. A. Lidar, I. L. Chung, and K. B. Whaley, *Phys. Rev. Lett.* **81**, 2594 (1998).
 - [15] A. Beige, D. Braun, B. Tregenna, and P. L. Knight, *Phys. Rev. Lett.* **85**, 1762 (2000).
 - [16] L. Campos Venuti, C. Degli Esposti Boschi, and M. Roncaglia, *Phys. Rev. Lett.* **99**, 060401 (2007).
 - [17] E. Manousakis, *Rev. Mod. Phys.* **63**, 1 (1991);
 - [18] M. Hase, and I. Terasaki, and K. Uchinokura, *Phys. Rev. Lett.* **70**, 3651 (1993).
 - [19] K. Hirakawa and Y. Kurogi, *Prog. Theor. Phys. Suppl.* **46**, 147 (1970); H. Yoshizawa and K. Hirakawa, *Phys. Rev. B* **21**, 2001 (1980).
 - [20] C. F. Hirjibehedin, *et al. Science* **312**, 1021 (2006).
 - [21] P. W. Anderson, *Basic Notions of Condensed Matter Physics* (Addison Wesley, New York, 1984).

- [22] G. Vidal, and R. F. Werner, Phys. Rev. A **65**, 032314 (2002).
- [23] W. K. Wootters, Phys. Rev. Lett. **80**, 2245 (1998).
- [24] A. Ferreira and J. M. B. Lopes dos Santos, Phys. Rev. A **77**, 034301 (2008).
- [25] L. Campos Venuti, S. M. Giampaolo, F. Illuminati, P. Zanardi, Phys. Rev. A **76**, 052328 (2007).
- [26] A. Auerbach, *Interacting Electrons and Quantum Magnetism* (Springer, New York, 1994).
- [27] S. R. White, R. M. Noack, and D. J. Scalapino, Phys. Rev. Lett. **73**, 886 (1994).
- [28] H.G. Evertz, Adv. in Physics, **52**, 1 (2003); S. Todo and K. Kato, Phys. Rev. Lett., **87**, 047203 (2001); S. Todo in *Condensed-Matter Physics*, edited by D.P. Landau, S.P. Lewis, and H.-B. Schuettler (Springer, Berlin, 2003), Vol. 15; F. Alet *et al.*, J. Phys. Soc. Jpn. Suppl. **74**, 30 (2005); A. F. Albuquerque *et al.*, J. Mag. Mag. Mat. **310**, 1187 (2007).
- [29] G. Chen, H-Q. Ding, and W. Goddard III, Phys. Rev. B **46**, 2933 (1992).
- [30] J. Carlson, Phys. Rev. B **40**, 846 (1989).
- [31] D. Loss and D. P. DiVincenzo, Phys. Rev. A **57**, 120 (1998); G. Burkard, D. Loss, and D. P. DiVincenzo, Phys. Rev. B **59**, 2070 (1999).
- [32] J. R. Schrieffer and P. A. Wolff, Phys. Rev. **149**, 491 (1966).
- [33] Aires Ferreira, Ph.D. Thesis. *The Quantum-Classical Boundary: from Opto-Mechanics to Solid-State* (Universidade do Porto, 2009), pre-print: arXiv: 0911.2217.